Hybrid asynchronous brain–computer interface for yes/no communication in patients with disorders of consciousness

Journal of Neural Engineering

PAPER

Hybrid asynchronous brain–computer interface for yes/no communication in patients with disorders of consciousness

Jianyong Huang[1,4], Lina Qiu[1,4], Qianmin Lin[2], Jun Xiao[3], Yuanqiu Huang[2], Haiyun Huang[3], Xinjie Zhou[2], Xiangyu Shi[3], Fei Wang[1,3], Yanbin He[2,*] and Jiahui Pan[1,3,*]

[1] School of Software, South China Normal University, Guangzhou 510630, People's Republic of China
[2] Traumatic Brain Injury Rehabilitation & Severe Rehabilitation Department, Guangdong Work Injury Rehabilitation Hospital, Guangzhou 510400, People's Republic of China
[3] Center for Brain Computer Interfaces and Brain Information Processing, South China University of Technology, Guangzhou 510640, People's Republic of China
[4] These authors contributed equally to the manuscript.
[*] Authors to whom any correspondence should be addressed.

E-mail: heyb_17@sina.com **and** panjiahui@m.scnu.edu.cn

Keywords: communication, disorder of consciousness, brain–computer interface, hybrid system, asynchronous detection, P300, steady-state visual evoked potential (SSVEP)

OPEN ACCESS

RECEIVED
28 October 2020

REVISED
2 March 2021

ACCEPTED FOR PUBLICATION
18 March 2021

PUBLISHED
6 April 2021

Abstract

Objective. For patients with disorders of consciousness (DOC), such as vegetative state (VS) and minimally conscious state (MCS), communication is challenging. Currently, the communication methods of DOC patients are limited to behavioral responses. However, patients with DOC cannot provide sufficient behavioral responses due to motor impairments and limited attention. In this study, we proposed a hybrid asynchronous brain–computer interface (BCI) system that provides a new communication channel for patients with DOC. *Approach.* Seven patients with DOC (3 VS and 4 MCS) and eleven healthy subjects participated in our experiment. Each subject was instructed to focus on the square with the Chinese words 'Yes' and 'No'. Then, the BCI system determined the target square with both P300 and steady-state visual evoked potential (SSVEP) detections. For the healthy group, we tested the performance of the hybrid system and the single-modality BCI system. *Main results.* All healthy subjects achieved significant accuracy (ranging from 72% to 100%) in both the hybrid system and the single modality system. The hybrid asynchronous BCI system outperformed the P300-only and SSVEP-only systems. Furthermore, we employed the asynchronous approach to dynamically collect the electroencephalography signal. Compared with the synchronous system, there was a 21% reduction in the average required rounds and a reduction of 105 s in the online experiment time. This asynchronous system was applied to detect the 'yes/no' communication function of seven patients with DOC, and the results showed that three of the patients (3 MCS) not only showed significant accuracies ($67 \pm 3\%$) in the online experiment, and their Coma Recovery Scale-Revised scores were also improved compared with the scores before the experiment. This result demonstrated that 3 of 7 patients were able to communicate using our hybrid asynchronous BCI system. *Significance.* This hybrid asynchronous BCI system can be used as a useful auxiliary bedside tool for simple communication with DOC patients.

1. Introduction

Disorders of consciousness (DOCs) are the most serious sequelae of brain injury and are characterized by deficits in consciousness and cognitive impairment, including coma, vegetative state (VS), minimally conscious state (MCS), and locked-in syndrome (LIS). Patients in a VS have no discrete localized motor control, cannot express comprehensible words and cannot open their eyes spontaneously to obey verbal commands [1–3], while MCS is characterized by inconsistent but reproducible signs of awareness through behavioral responses [4]. Patients who have been in a VS for a long period of time are classified

as persistent vegetative patients [5]. The LIS patients, who are characterized by anarthria and quadriplegia, with generally preserved cognition, must be distinguished from VS and MCS patients [3]. Patients with different consciousness disorders have different levels of consciousness. Accurate detection of consciousness is the key to the diagnosis and treatment of patients with DOC. Currently, the most commonly used methods to assess the state of consciousness of DOC patients are behavior scoring scales, such as the JFK Coma Recovery Scale-Revised (JFK CRS-R) [6, 7]. However, this behavior-based assessment method has a high rate of misdiagnosis (37%–43%) [2, 8, 9], especially in the assessment of VS and MCS. For example, in a study of 137 patients, 24.7% of the patients who were assessed as clinical VS patients in a single CRS-R behavior evaluation were actually MCS patients, and the repeated CRS-R evaluation results showed that the misdiagnosis rate of MCS was 38.2% [10]. Therefore, it is difficult to accurately assess a patient's level of consciousness based only on the patient's behavior. It is meaningful and necessary to explore nonbehavior-based and objective methods to diagnose patients' consciousness and to assess the clinical prognosis of patients with DOC. Furthermore, laws and ethics related to the treatment of patients (including VS and MCS patients) are also very important issues. The permanent VS is legally recognized as dead in only a few legal systems. Some researchers hold that it is illegal or unethical to withdraw life-sustaining treatment from patients with prolonged DOC and that patients should receive continued care as long as there is a chance of recovery [11].

Recently, several studies have shown the potential of brain–computer interfaces (BCIs) to detect residual cognitive function in patients with DOC. In our previous studies [12–14], we presented three hybrid BCIs for awareness detection in patients with DOC, including two hybrid BCIs combining P300 and steady-state visual evoked potentials (SSVEPs) and an audiovisual BCI. For instance, in [12], a visual hybrid BCI combining P300 and SSVEPs was used to detect awareness in eight patients with DOC (four VS, three MCS, and one LIS), and command-following behavior was demonstrated in three patients (one VS, one MCS, and one LIS). It is worth noting that the cognitive ability of DOC patients is generally lower than that of healthy subjects, and they are prone to fatigue and lack of concentration, making it difficult to complete long-duration experiments. Therefore, the BCI accuracy of patients with DOC is generally lower than that of healthy subjects. It is a necessary and challenging task to improve BCI performance in patients with DOC. One possible improvement method is to optimize the BCI control strategy such that as many DOC patients as possible can use BCIs, provided that they have consciousness to some extent.

The BCI control strategy can be asynchronous or synchronous. Asynchronous BCIs are user-friendly systems that can detect whether the user intends to send a control command [15]. They allow the user to freely switch states, thereby achieving more natural control [16–18]. When asynchronous BCIs are applied to DOC patients, online feedback results during the limited attention span could be outputted in a dynamic period. This approach may be promising to maximize the patients' chances to provide evidence of residual brain functions to examiners. To the best of our knowledge, there is no study on asynchronous BCIs for DOC patients.

Communication is a basic ability that patients with DOC generally lack and urgently need. Some recent studies have demonstrated the potential of BCIs to communicate with DOC patients. Cruse *et al* instructed a group of 16 VS patients to perform two motor imagery tasks; specifically, they were asked to imagine movements of their right hand and toes on command. Their results showed that 3 of the 16 VS patients were able to repeatedly and reliably generate appropriate electroencephalography (EEG) responses to two distinct commands with an accuracy of 78%, which provides hope for future bedside communication with VS patients [19]. However, the obtained results were challenged by subsequent independent analyses, which illustrates the challenge of proposing a reliable BCI technology for clinical use in patients with DOC. Lulé *et al* tested a 4-choice (Yes, No, Stop and Go) auditory oddball EEG-BCI in 16 healthy subjects and 18 DOC patients (3 VS, 13 MCS, and 2 LIS), and found that 13 healthy subjects (with an average correct response rate of 73 $\pm$ 23%) and one LIS patient (the correct response rate is 60%) were able to communicate with the BCI, indicating that a BCI has the potential to serve as a 'yes-no' spelling device for functional interactive communication [20]. In our previous study [14], Wang *et al* proposed an audiovisual BCI communication system to supplement the JFK CRS-R with a 'yes-no' choice system for 13 patients (8 VS and 5 MCS) to perform BCI-based assessment and found that 8 of the 13 patients with DOC showed responsive results, with an average accuracy of 77.3%. In the above studies, the BCIs developed for DOC patients were all synchronous BCIs based on a single modality (such as P300 or motor imagery). It is difficult to maintain their limited attention during the fixed period for DOC patients. The use of BCIs to detect the communication ability of DOC patients is still in its infancy, and alternative hybrid asynchronous BCI systems (i.e. asynchronous detection directly combining information from multiple EEG measurements) may be promising to improve brain activity detection in this very challenging patient population.

The performance of hybrid BCIs that combine two or more different types of brain signals (e.g. P300 potentials and SSVEPs) has been validated in recent

studies [21]. In our previous study [13], we proposed a hybrid system based on P300 and SSVEPs. Our results showed that the performance achieved by the hybrid BCI system was significantly enhanced over that of the unimodal BCI, but we employed only simple fusion at the decision level by summing the P300 and SSVEP scores. Many fusion methods have recently been proposed to further improve the performance of hybrid systems [22, 23]. For example, Yin *et al* developed a maximum-probability estimation fusion approach based on the combination of P300 and SSVEPs, and an average accuracy of 95.18% was achieved [24]. These studies indicated that the optimized fusion method could improve the performance of the hybrid BCI system.

Considering the above issues, in this paper, we developed a hybrid asynchronous BCI system for communicating with DOC patients. A total of 11 healthy subjects and seven DOC patients participated in the experiment. The state of consciousness of all patients was evaluated using the CRS-R during the week before the experiment. In this system, two flickering squares with the Chinese words 'Yes' and 'No' and corresponding square frames were used as the visual stimuli and feedback. P300 and SSVEPs were collected from the flashing (appearance and disappearance) of the square frames and the flickering of the square, respectively. This system combined P300 and SSVEP detection to determine whether the patient focuses on the instructed target square of the answer on the graphical user interface (GUI). A linear support vector machine (LSVM) with a linear kernel was applied for the fusion of P300 and SSVEPs at the score level. Due to the low concentration of DOC patients, we introduced a Bayesian framework to dynamically control the data collection of the BCI system. Our results in 11 healthy control subjects showed that the asynchronous hybrid BCI system outperformed the P300-only and SSVEP-only systems. Furthermore, for the patient group, 3 of 7 patients achieved significant accuracies in the online experiment (classification accuracy 64%–70%), indicating that three DOC patients were able to communicate with the BCI system. To the best of our knowledge, this study is the first to test a hybrid asynchronous BCI for communicating with DOC patients.

2. Materials and method

The definitions and related descriptions of key terms used in this section are as follows:

Block: For each subject, the online test experimental run contained five blocks, each containing ten trials. Due to the limited attention of DOC patients, different blocks were performed on different days.

Trial: Each trial was divided into four phases: instruction, stimulation, feedback, and rest. The subjects were instructed to answer yes/no questions by focusing on the target square, and to count the number of times the frame of the corresponding square flashed until feedback emerged on the screen.

Round: During the stimulation in each trial, one round indicated that the square frame on the left and right sides flashed once, or the square flickered for 2 s.

Epoch: The unit length of P300 and SSVEP detection data. For P300 detection, the epoch meant the EEG signal 0–800 ms after a square frame flash. For SSVEP detection, the epoch corresponded to the 2000 ms EEG signal during the flickering period in the stimulation phase of each trial.

2.1. Subjects

This study was approved by the ethics committee of Liuhuaqiao Hospital, which complies with the Code of Ethics of the World Medical Association (Declaration of Helsinki). Seven patients with severe brain damage (mean ± SD = 39.86 ± 19.14 years; six men) and 11 healthy volunteers (mean ± SD = 29.67 ± 2.54 years) participated in this experiment. All subjects (or family members of patients) were informed of the experimental details and signed a written informed consent form before the experiment. All subjects had no history of impaired vision or hearing. The seven patients included three VS and four MCS patients. Detailed information for the three VS and four MCS patients is shown in table 2. Their clinical diagnosis was based on the CRS-R, which comprises six subscales for auditory, visual, motor, oromotor, communication, and arousal functions [6].

2.2. Data acquisition system

In the experiment, the NuAmps device (Compumedics, Neuroscan, Abbotsford, Australia) was used to collect EEG signals of subjects. The reference electrode of the EEG signal was placed on the right mastoid, and the ground electrode was located at the 'Fpz' position. During the experiment, the subjects wear the electrode cap while staying awake. A display screen was placed approximately 0.5 m in front of the subject and adjusted to the best viewing angle. There were a total of nine measurement channels, namely, 'CPz', 'P7', 'P3', 'Pz', 'P4', 'P8', 'O1', 'Oz' and 'O2', of the standard 10–20 system [25]. The impedance of all electrodes was kept below 5 kΩ, and the sampling rate of EEG signals was 250 Hz.

2.3. Graphical user interface and BCI paradigm

The GUI used in this experiment is shown in figure 1. Two squares and two corresponding square frames were used as the stimulus source to generate SSVEP and P300 signals: one square with the Chinese character 'Yes', and the other with the Chinese character 'No'. Each square (size: 6.24 × 6.92 cm) was placed in the center of a white square frame (size: 8.04 × 8.86 cm,

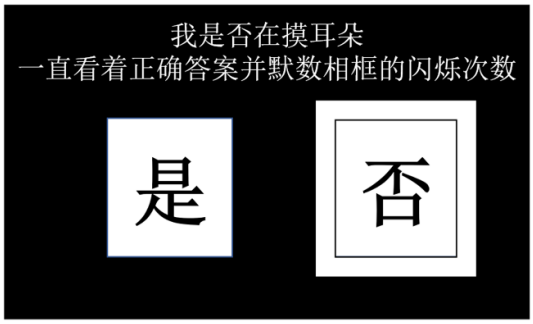

Figure 1. GUI of the BCI system. In the GUI, two squares with Chinese characters 'Yes' and 'No' are respectively placed in the center of the two white square frames on the left and right. In each trial, the two squares were randomly displayed on the left and right sides at a frequency of 6.0 Hz and 7.5 Hz, and the square frame also appeared around the squares in random order.

margin width: 0.9 cm). The two squares were randomly displayed on the left and right sides of the screen.

The BCI paradigm is shown in figure 2. The display screen first prompted the trial to start with text and voice and then randomly displayed the preset text instructions, such as 'Am I touching my ear now? Please focus on the square of the answer and count the times that the frame flashes'. The subjects were instructed to focus on the target answer square of the question and count the number of flashes of the corresponding square frame. After the instruction phase lasting 8 s, the two squares were embedded in a static frame and flickered at different frequencies (the flashing frequencies of the left and right squares were 6.0 and 7.5 Hz, respectively) to evoke the SSVEPs related to the left/right square (i.e. stimulus frequency-driven EEG responses). Meanwhile, the square frame flashed (from appearing to disappearing) randomly on the left and right sides of the screen, with each flash lasting 200 ms, and the interval between two consecutive appearances was 800 ms. Thus, one round of the intensification of the two square frames lasted 2000 ms, where one round was defined as a complete cycle in which each square frame flashed once on the left and right sides. These flashes of the left/right square frame would evoke the P300 potentials related to the left/right square-frame (i.e. stimulus oddball-driven EEG responses). The left and right square frames were successively flashed five times in a trial. The total time of the stimulation phase was set as 10 s. Then, the feedback of this trial was displayed on the screen.

Before the start of the experiment, the subjects were instructed to avoid any type of muscle movement and eye blinking during the trial. During the experiment, the subject's performance was carefully observed by a special observer. If the subject closed his/her eyes for more than 4 s or moved his/her body continuously (e.g. coughing) during the trial, the trial was discarded and the next trial was not started until the subject showed a prolonged spontaneous reawakening. In this study, an average of 4.8% of the number of trials per patient was eliminated.

2.4. Data processing and algorithm

The data processing procedure included P300 and SSVEP detection. Figure 3 shows the data processing process of P300 and SSVEP detection.

2.4.1. P300 detection

In the training period, each subject performed a training run with ten trials. In each trial, the epochs (i.e.0–800 ms after the intensification of the square frame) of the EEG signal were extracted from each channel of each square frame. A baseline correction of 100 ms prior to the stimulus was used for all epochs. After the 0.1–20 Hz bandpass filtering, we downsampled all data at a rate of 5 to obtain a data vector with a final sampling rate of 50 Hz. The epochs of all nine selected channels were then concatenated to generate feature vectors. In the training session, we averaged five rounds (flashing) of data in one trial. All feature vectors were normalized and mapped into the range [0, 1]. Finally, using the feature vectors and their labels (+1 and −1), if the subject focused on the target square frame, the label was +1; otherwise, the label was −1. A support vector machine (SVM) classifier was trained for each subject for asynchronous P300 detection. We used leave-one-out cross-validation to identify the SVM classifier's generalization error for the dataset. Specifically, one trial in each fold was used for testing, and the others were used for training. The cross-validation accuracies for healthy subjects ranged from 80% to 100%. In this system, SVMs were implemented by LIBSVM, a library for SVMs [26].

Furthermore, a sliding window strategy was adopted in this study. The length of the sliding window was 6 s, which corresponds to three rounds of intensification of the two square frames. In other words, for asynchronous P300 detection, the feature vectors were obtained by averaging the last three rounds (i.e. 6 s) from the current time point. Figure 4 shows the framework of asynchronous detection. With the well-trained SVM classifier, two SVM scores $\left(\text{score}_i^1, \text{score}_i^2\right)$ were obtained in each trial and used for dynamic stopping.

2.4.2. SSVEP detection

Canonical correlation analysis (CCA) is a common analysis method for SSVEP-based BCIs [27–29], which aims to identify a pair of linear combinations to maximize the correlation between two canonical variables. CCA extends the ordinary correlation between the two sets of data. We assumed that the

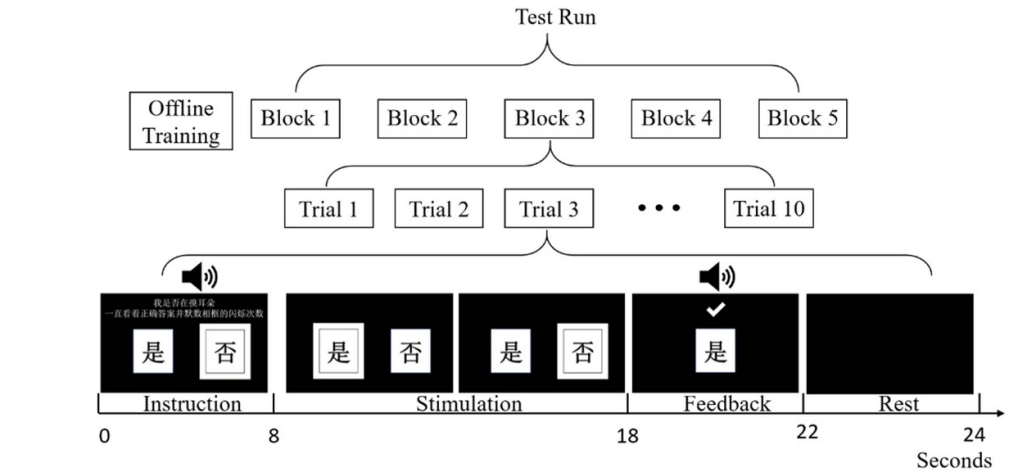

Figure 2. The experimental paradigm of the test run. The test run contains a total of five blocks, and each block contains ten trials. Each trial started with the visual and auditory instructions, and two squares were then displayed on the left and right sides of the screen. Subjects were asked to focus on the target square. Finally, auditory and visual feedback was presented.

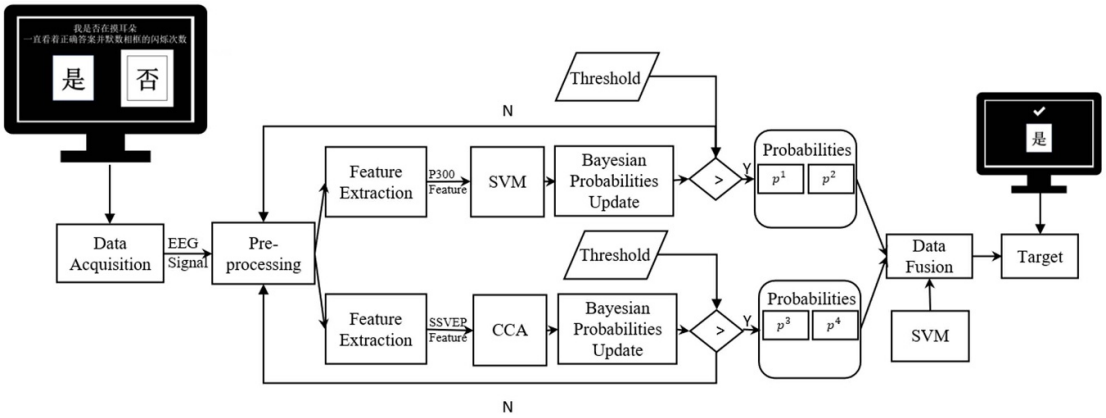

Figure 3. The data processing procedure of P300 and SSVEP detection. EEG signals were collected from the data acquisition system and then input into two different data processing procedures, one for P300 detection and the other for SSVEP detection. During P300 and SSVEP detection, we introduced a Bayesian framework to update the probability. In each trial, the response of the classifier was calculated to estimate the target probability (p^1 and p^3) and nontarget probability (p^2 and p^4), and the target probability was compared with the threshold. Then, the probability from the classifier was input into the SVM model for data fusion. Finally, the target answer that the subjects focused on was displayed on the screen as feedback.

linear combinations of two multidimensional variables X and Y are $x = X^T W_X$ and $y = Y^T W_Y$, respectively. CCA finds the weight vectors W_X and W_Y by solving the following problem to maximize the correlation between x and y:

$$\max_{W_X, W_Y} \rho(x,y) = \frac{E\left[x^T y\right]}{\sqrt{E\left[x^T x\right] E\left[y^T y\right]}} = \frac{E\left[W_X^T X\, Y^T W_Y\right]}{\sqrt{E\left[W_X^T X\, X^T\, W_X\right] E\left[W_Y^T\, Y\, Y^T W_Y\right]}}. \quad (1)$$

The maximum of ρ with respect to W_X and W_Y is the maximum canonical correlation. Projections to W_X and W_Y, that is, i.e. X and Y, are called canonical variants. Here, X represents the set of multichannel EEG signals, and Y represents the set of reference signals with the same length as X. Lin *et al* first used the CCA method to detect multichannel SSVEP-based BCIs [30]. In their paper, the reference signal Y_f was set as follows:

$$Y_f = \begin{bmatrix} \sin 2\pi ft \\ \cos 2\pi ft \\ \cdots \\ \sin 2\pi N_h ft \\ \cos 2\pi N_h ft \end{bmatrix}, t = \frac{1}{f_s}, \frac{2}{f_s}, \ldots, \frac{N}{f_s}, \quad (2)$$

where f is the target frequency, N_h is the number of harmonics, and N is the number of sampling points. To identify the frequency of the SSVEPs, we used the CCA method to calculate the canonical correlation between the multichannel EEG signals and the reference signals at each stimulus frequency and then selected the frequency of the reference signals with the maximal correlation as the frequency of SSVEPs.

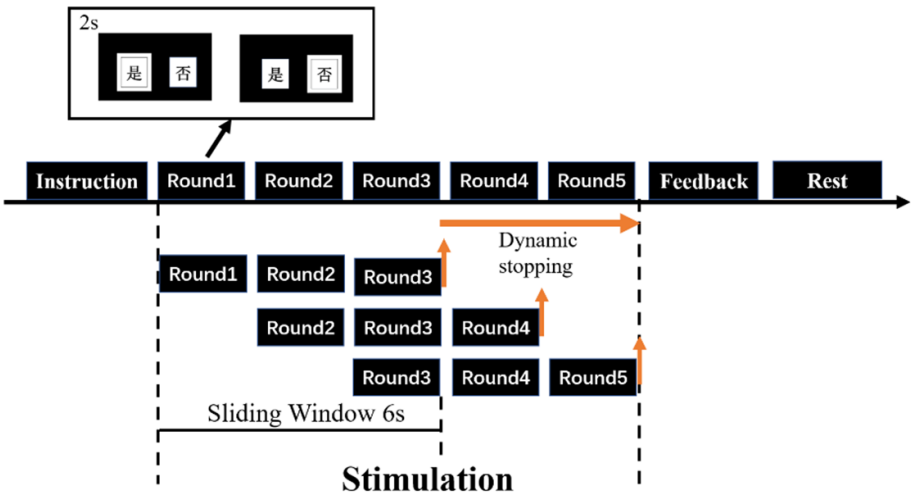

Figure 4. The framework of asynchronous detection in each trial. The length of the sliding window was set to 6 s (corresponding to three rounds). Starting from the end of the third round, asynchronous detection was performed every round (corresponding to 2 s).

Based on a previous study, Nakanishi proposed a multichannel approach that incorporated CCA and SSVEP training data in an SSVEP-based BCI [31]. In that proposed method, the training reference signal $\hat{X}$ was obtained by the training set X and three canonical coefficients: (a) $W_x\left(X\hat{X}\right)$, between the test set X and the reference signal; (b) $W_x\left(XY_f\right)$ between the test set X and the sine-cosine reference signal Y_f; and (c) $W_x\left(\hat{X}Y_f\right)$, between the training reference signal $\hat{X}$ and the sine-cosine reference signal Y_f. In this study, the CCA classifier was used to build a correlation vector ρ, which is defined as follows:

$$r=\begin{bmatrix} r(1) \\ r(2) \\ r(3) \\ r(4) \end{bmatrix}=\begin{Bmatrix} r\left(X^T, Y_f^T\right) \\ r\left(X^T W_x\left(X\hat{X}\right), \hat{X}^T W_x\left(X\hat{X}\right)\right) \\ r\left(X^T W_x\left(XY_f\right), \hat{X}^T W_x\left(XY_f\right)\right) \\ r\left(X^T W_x\left(\hat{X}Y_f\right), \hat{X}^T W_x\left(\hat{X}Y_f\right)\right) \end{Bmatrix}, \tag{3}$$

where $r(a, b)$ indicates the correlation coefficient between a and b. To combine these correlation values, we used the weight correlation coefficient $\tilde{r}$ as the final feature value for target identification:

$$\tilde{r}=\sum_{i=1}^{4}\operatorname{sign}(r_i)\cdot {r_i}^2, \tag{4}$$

where sign() is used to retain the discriminative information of the negative correlation coefficients between the test set and the training reference signals.

In this SSVEP detection, all EEG signals were band-pass filtered between 3 Hz and 20 Hz. In the offline training phase, the total flickering time of two squares on both sides (left and right) was 10 s. We first extracted epochs of the EEG signal from each channel for each square. The epochs correspond to the 10 s EEG signal during the total flickering period (2500 data points) in the stimulation phase of each trial. Then, we averaged these data and concatenated the epochs of all channels to generate feature vectors. Finally, we used the CCA classifier with training data [31] as the classifier. The feature vectors were used to train a CCA classifier for each subject. Furthermore, we performed leave-one-out cross-validation. In each fold, the data of one trial were used for testing, while the data for other trials were used for training.

In the online experiment, SSVEP detection was performed every 2 s starting from 6 s. First, the EEG signals were filtered in the range of 3–20 Hz. Then, we extracted the segment of EEG signals from each channel for each square in the 6 s period (1500 data points, corresponding to the length of a sliding window) before the current time point. Finally, all segments extracted from the selected channels were concatenated to generate feature vectors. The feature vectors were calculated to obtain two scores (score_i^3, score_i^4) for dynamic stopping, where score_i^3 corresponds to flashing on the left side, score_i^4 corresponds to flashing on the right side, and i is the trial index. We determined the target by the following formula:

$$T_{\text{ssvep}}=\arg\max_{i=1\ldots n}\left(\text{score}_i^3, \text{score}_i^4\right). \tag{5}$$

2.4.3. Dynamic stopping

In the online phase, the Bayesian asynchronous approach was applied for dynamic stopping. First,the classifier response scores for target and nontarget flashes were grouped. Then, the grouped classifier scores were scaled, and smoothed using kernel density estimation, and finally the likelihood probability density functions (pdfs) of the target response $p(y_i|H_{+1})$ and nontarget response $p(y_i|H_{-1})$ were generated, where H_1 corresponds to the space of the target response $(+1)$, and H_{-1} corresponds to the space of nontarget response (-1).

The pdfs were used to update the probability of each epoch in the Bayesian framework. Each flash was assigned an initialization probability, $p(A)$. In the

online experiment, two squares flashed randomly on the left and right, and all flashes had the same probability of being the target, which was $p(A) = \frac{1}{N}$, where N is the total number of flashes. In this study, N was set to 2. In each new round of flashing, the response probability was updated via Bayesian inference:

$$p(A|X) = \frac{p(X|A)\,p(A)}{p(X)}. \tag{6}$$

Given the current classifier response X, $p(A|X)$ is the posterior probability of each answer A as the target answer; $p(X|A)$ is the probability of the classifier response; $p(A)$ is the prior probability of flashing; and $p(X)$ is the total probability of the classifier response. Due to the law of total probability [32], the denominator can be replaced as follows; specifically, we changed the total probability to the sum of the probabilities of each flash

$$p(A|X) = \frac{p(X|A)\,p(A)}{\sum_A p(X|A)\,p(A)}. \tag{7}$$

In this study, we proposed a 'YES/NO' communication system. The goal of each round of the experiment was to find the target answer (i.e. Yes or No). However, the classifier response of the target square or square frame is not the final answer. We used the following method to transform the classifier response to the probability of the final answer:

$$p(\text{Target}) = \frac{pc * \text{pdf}(\text{Target})}{(1-pc) * \text{pdf}(\text{NonTarget}) + pc * \text{pdf}(\text{Target})}. \tag{8}$$

After each Bayesian probability update, the probability of each flash was compared with a threshold. The threshold indicates the confidence at which the correct character was chosen and is defined by the following formula:

$$\text{threshold} = m - z\frac{s}{\sqrt{n}} \tag{9}$$

where m is the average probability of the target answer; z is the chosen Z-value (1.645 for 90%); s is the standard deviation of the probability of the target answer; and n is the total number of training trials. This threshold indicates the confidence that the answer is correct based on signal-to-noise ratios. In this study, the threshold was represented by a 90% confidence interval of target probabilities obtained in synchronous mode. The lower the threshold, the fewer data are required and the more errors are generated, thereby reducing accuracy. Lower accuracy may result in a higher communication rate [33]. Therefore, accuracy can be improved by selecting an appropriate threshold.

2.4.4. Data fusion

Multimodal systems have been demonstrated to have better recognition performance than unimodal systems by using fusion approaches at various levels, such as the feature, score, or decision level. However, since P300 and SSVEP features exist in the time and frequency domains (different feature spaces), respectively, it is difficult to utilize the fusion approach at the feature level. Therefore, we performed a fusion approach based on the P300 and SSVEP score levels. Specifically, after the Bayesian model updated answer probabilities from P300 and SSVEP detection, we concatenated the above P300 probabilities and SSVEP probabilities to build a fusion feature vector $X = (x_1, x_2, \ldots, x_n)$, where x_n is the vector of the n_{th} trial,

$$x_n = \begin{bmatrix} p_i^1 \\ p_i^2 \\ p_i^3 \\ p_i^4 \end{bmatrix}. \tag{10}$$

The feature vector with target label $Y = \{y_1, y_2, \ldots, y_n\}$ was input into the classifier:

$$(x_1, y_1), \cdots (x_n, y_n) \in R^n \times (+1, -1). \tag{11}$$

Here, the LSVM was used as the classifier. SVM usually constructs a hyperplane in a high-dimensional or infinite-dimensional space to minimize the classification error [34]. The target of the trial could be predicted by solving the following problem:

$$f(x) = w \cdot x + b, \tag{12}$$

where w is the weight vector. After training the SVM model with offline data, the feature vector was input into the SVM model. Then, we predicted the label of the target by maximizing the SVM decision value:

$$T_{\text{fusion}} = \arg\max_{i=1\ldots n} \left(\text{score}_i^1, \text{score}_i^{-1}\right). \tag{13}$$

3. Experiment

During the experiment, the subject sat in a comfortable wheelchair about 0.5 m away from a 22 inch LED display. Before the experiment, the subjects were initially screened and the experimental procedures were explained to the subject or their family.

In this experiment, we tested the online performance of healthy participants and patients with DOC in an asynchronous system using the SSVEP- and P300-based hybrid system. The experiment was divided into two steps.

Step I, offline training: before conducting an online experiment, each subject performed a training run consisting of ten trials. The training paradigm is shown in figure 1. The two squares of answers flickered in different frequencies, and the square

frames also flashed in random order, each appearance lasting for 200 ms, and once every 800 ms. There were five rounds in each trial. Each trial started with an audiovisual instruction of about 8 s. During the instruction, the subject encountered a situation question, such as 'Am I touching my nose right now' or 'Am I touching my right ear right now'. The subjects were instructed to pay attention to the square indicating the answer and count the number of times the corresponding square frame flashed. The data from the training phase were used to train the initial P300 and SSVEP models. For P300 detection, an SVM model with RBF kernel functions was trained on these data. For SSVEP detection, a CCA model was trained.

Step II, online testing: similar to Step I, all subjects were asked to focus on the screen to select the answer to the preset question, but the difference was that the online testing phase used an asynchronous system. The experimental paradigm of the test run is shown in figure 2. The test run contained five blocks, each consisting of ten trials. The asynchronous framework is shown in figure 3. In each trial, after the question appeared on the screen, the subject was instructed to stare at the square and count the number of times the corresponding square frame appeared. After instructions were given, the system detected the state of the subject and provided the detected answer. Then, another question in the next trial was displayed on the screen 2 s later. The EEG data obtained in the offline training phase were used to train the classifier model. After the data processing above, the P300 and SSVEP classification models were updated.

In the online testing phase, the data from the subjects were grouped into target and nontarget responses and then classified according to the model obtained in the training phase. For each trial, the EEG epochs were extracted from the 6 s period (1500 data points, corresponding to the length of a sliding window) before the current time point for each channel. After P300 and SSVEP detection simultaneously, the P300 and SSVEP scores were used to calculate the probabilities of the target based on the Bayesian framework. Then, the Bayesian probabilities were compared with the threshold to determine if the data collected from the current sliding window could be selected. Finally, we concatenated the above P300 probabilities and SSVEP probabilities to build a fusion feature vector. The feature vector was input into an SVM model, and the target was determined as the feedback of each trial.

We used accuracy to reflect the ratio of all correct responses (hits) to the total number of trials presented. To verify the significance of this accuracy rate, we also conducted a statistical analysis, as described below [35]:

$$\chi^2 = \sum_{i=1}^{k} \frac{(fo_i - fe_i)^2}{fe_i}, \tag{14}$$

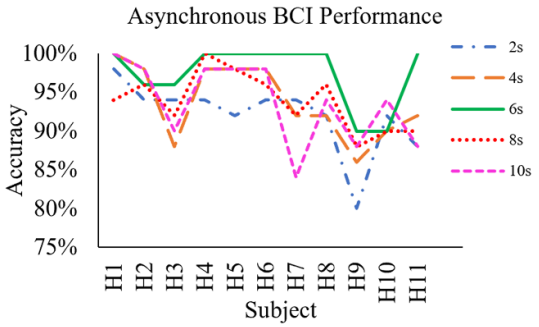

Figure 5. The sliding window performance for the healthy control group in the asynchronous system. The length of the sliding window was set at 2, 4, 6, 8, and 10 s. The data were collected from the offline experiment for 11 healthy subjects.

where fo_i and fe_i are the observed frequency and expected frequency of the ith class ($i = 1, 2, \ldots k$), respectively. In this study, the observations were divided into two classes (hits and misses). Specifically, fo_1 and fo_2 were the observed numbers of hits and misses, respectively, and fe_1 and fe_2 represented the expected numbers of hits and misses, respectively. The degree of freedom was 1 for our two-choice BCI. For example, when 50 trials are performed per round in a two-choice paradigm, there may be 25 hits and 25 misses by chance. It was assumed that the difference was significant when $p \leqslant 0.05$. The χ^2 value we obtained was 3.84 (degrees of freedom was set to 1), which is equivalent to 32 hits in 50 trials with an accuracy of 64%.

4. Results

We tested the performance of the asynchronous system in sliding windows of different sizes. For 11 healthy subjects, each subject was asked to perform 50 trials. The size of the sliding window in different asynchronous systems was set to 2, 4, 6, 8, and 10 s. As shown in figure 5, when the size of the sliding window was set to 6 s, the healthy subjects showed better performance in the asynchronous system.

Table 1 summarizes the accuracy rates of the online and offline experiments for healthy subjects. The online accuracy of hybrid BCIs for 11 healthy subjects (ranging from 90% to 100%) was higher than the chance level of 64%, and 9 of them (H1, H2, H3, H4, H5, H6, H7, H8, and H11) even achieved an accuracy above 95%. In the synchronous system, each trial square flashed for five rounds (2 s per round), while the average number of rounds in the asynchronous system was less than five rounds, i.e. 3.87 rounds. To demonstrate that the multimodal system performs better than the single-modality system, the offline accuracies of the P300- or SSVEP-only based system for all healthy subjects are also presented in table 1. For all healthy subjects, the accuracy based on the single-modality system was also higher than

Table 1. The accuracy of the online and offline experiments for 11 healthy subjects.

Subjects	P300 + SSVEP (50 trials)	Offline accuracy rates (50 trials)		Average rounds in asynchronous system
		P300	SSVEP	
H1	100%	74%	94%	4.06
H2	96%	90%	74%	4.46
H3	96%	86%	94%	3.10
H4	100%	76%	94%	3.33
H5	100%	100%	100%	4.00
H6	100%	100%	100%	3.00
H7	100%	84%	84%	4.16
H8	100%	100%	100%	3.10
H9	90%	72%	98%	4.30
H10	90%	78%	88%	4.46
H11	100%	88%	76%	3.50
Average	97.45 ± 3.82%	86.18 ± 10.07%	91.09 ± 9.00%	3.77 ± 0.55

Note: The value of average rounds indicates the average number of rounds in each trial. In the synchronous system, the number of average rounds was fixed at 5.

Table 2. The online accuracy in the hybrid BCI-based experiment and the CRS-R scores for all patients.

Patients	50%s	Age	Gender	Accuracy rates	CRS-R scores (subscores)		Average rounds
					Before the experiment	After the experiment	
P1	VS	22	F	50%	6 (1-0-2-1-0-2)	6 (1-0-2-1-0-2)	4.00
P2	VS	19	M	58%	7 (1-1-2-1-0-2)	7 (1-1-2-1-0-2)	3.77
P3	VS	53	M	56%	6 (1-1-2-0-0-2)	13 (2-3-5-0-0-3)	3.00
P4	MCS	42	M	56%	8 (1-2-2-1-0-2)	10 (2-2-3-1-0-2)	3.66
P5	MCS	47	M	**66%**	10 (1-3-3-1-0-2)	15 (4-5-2-2-0-2)	4.20
P6	MCS	59	M	**70%**	14 (1-3-3-3-2-2)	20 (4-5-3-3-2-3)	4.70
P7	MCS	37	M	**64%**	9 (2-2-3-0-0-2)	12 (3-3-4-0-0-2)	4.16

Note: Coma Recovery Scale-Revised subscales: auditory, visual, motor, oromotor, communication and arousal functions.
The accuracies that were significantly higher than the chance level (64%) are highlighted in bold.

the chance level of 64%. However, the average online accuracy rates obtained based on the hybrid system were higher than those of the P300-only and SSVEP-only based systems.

The online accuracy rate in the hybrid system and the CRS-R scores of each patient (including 3 VS and 4 MCS) are listed in table 2. The accuracy rate of the three MCS patients (P5, P6, and P7) in the hybrid asynchronous system was higher than chance (i.e. $\geqslant$64%), and the average accuracy (standard deviation) was 67 ± 3%, while the accuracy of the other patients (3 VS and 1 MCS) was lower than 64%. Furthermore, the three patients (i.e. P5, P6 and P7) with significant accuracy in the experiment all showed improved scores in the CRS-R evaluation results after the experiment.

We extracted P300 event-related potential (ERP) waveforms from three subjects (P5, P6, and P7) with online accuracies higher than chance level, and ERP waveforms from 0 to 800 ms were extracted by time-locked averaging of the EEG signals across all 50 trials in the test run. Figure 6 shows the average EEG signal amplitudes of the selected channels (i.e. 'CPz', 'Pz' and 'Oz') for these three patients and healthy controls (H1). Obvious P300 responses to the target stimuli were observed in the waveforms of three patients by using the BCI system.

Considering the target stimuli that flickered randomly on the left or the right side of the screen in each trial, the EEG signal of total trials of each subject was grouped into two parts based on the frequency of the target stimuli in each group: 6 and 7.5 Hz, respectively. In addition, for patient subjects P5, P6, P7 and the healthy subject H1, we used discrete Fourier transform to obtain two average power density spectrum curves corresponding to the target squares appearing on the left and right sides of the GUI from the EEG signals of all the trials, as shown in figure 7(A). Specifically, for each subject, the EEG signals with a 10 s period were extracted from the occipital electrodes ('O1', 'Oz', and 'O2'). During the Fourier transform, a zero-padding method was used to increase the number of data points to 1024 (a power of 2).

For the ith subject, the power density spectrum of the jth group is $P\left(f_i^j\right)$, where f_i^j is the flickering frequency. The power ratio of the jth group for the ith subject is defined as

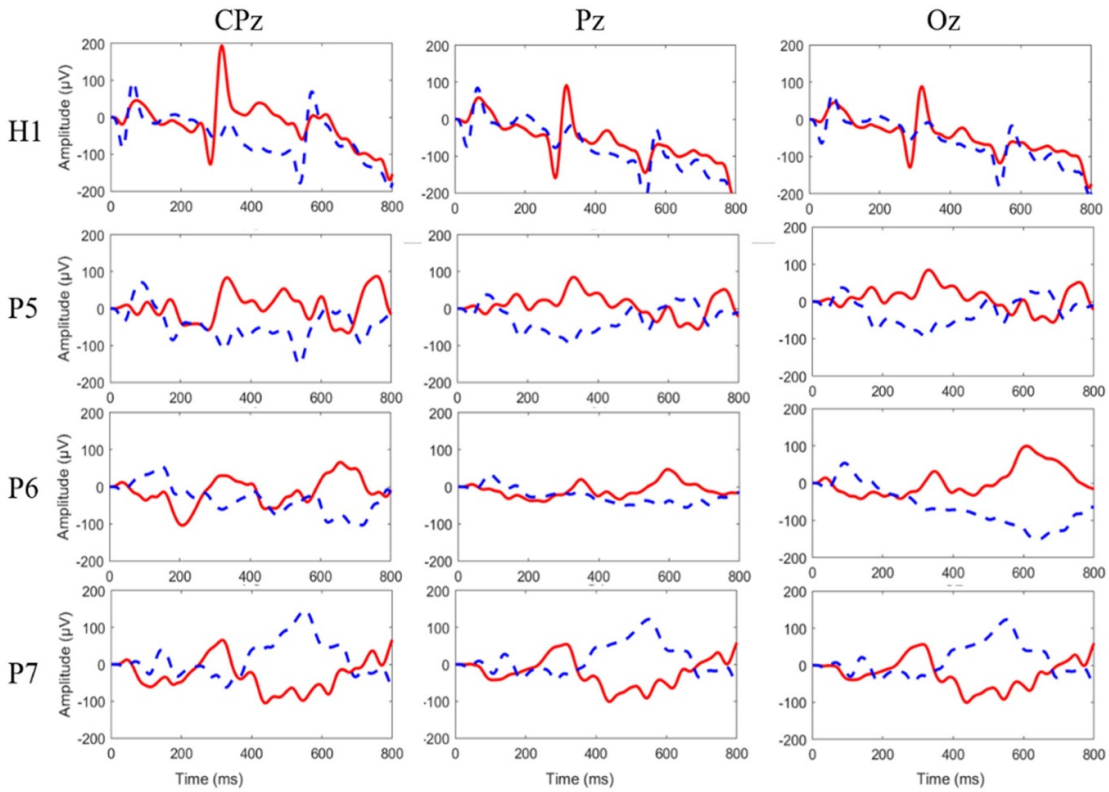

Figure 6. The grand-average P300 ERP waveforms from subjects in selected channels ('CPz', 'Pz' and 'Oz'). We extracted data from selected channels and averaged the data across 50 trials. The solid red curves containing P300 responses and the dashed blue curves without P300 responses indicate the target and nontarget square frames, respectively.

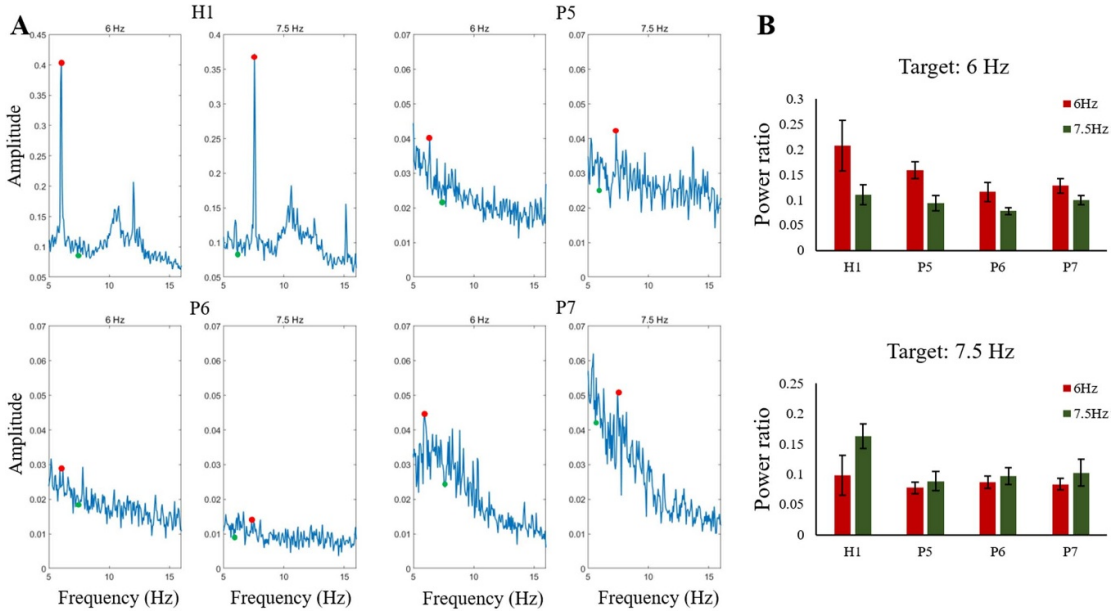

Figure 7. (A) Average power density spectra of EEG signals from the occipital channels ('O1', 'Oz' and 'O2') in all trials for subjects (H1, P5, P6, and P7). The red dot and the green dot correspond to the flickering frequency of the target square and the non-target square, respectively. The target frequencies of 6 Hz and 7.5 Hz corresponded to the flashed frequencies of the target squares on the left and right sides of the GUI, respectively. (B) The power ratio between the wide band and narrow band for subjects H1, P5, P6, and P7. For each subject, trials included two groups: 6 and 7.5 Hz, which represented the frequency of the target stimuli in each trial. We averaged the power ratio of the total trial in each group for each subject. Error bars = standard deviation.

$$\delta_i^j = \frac{[P(f)]_{f\in[f_i^j-f_n,\,f_i^j+f_n]}}{[P(f)]_{f\in[f_i^j-f_w,\,f_i^j+f_w]}} \tag{15}$$

where $[P(f)]_{f\in[f_i^j-f_n,\,f_i^j+f_n]}$ is the mean power in the narrow band $\left[f_i^j-f_n, f_i^j+f_n\right]$ and $[P(f)]_{f\in[f_i^j-f_w,\,f_i^j+f_w]}$ is the mean power in the wide band $\left[f_i^j-f_w, f_i^j+f_w\right]$. Here, f_n and f_w were set to 0.1 and 1 Hz, respectively.

Furthermore, we calculate the power ratio between the wide band and the narrow band for subjects H1, P5, P6, and P7 in figure 7(B).

5. Discussion

The communication ability of patients with DOC is highly important for auxiliary clinical diagnosis. Here, we proposed a hybrid BCI system for consciousness detection and communication in patients with DOC. Eleven healthy subjects and seven patients participated in our experiment. The accuracy rates of all 11 healthy subjects were higher than the chance level (i.e. 64%) with hybrid asynchronous BCIs, which were considered significant [35]. Nine of these healthy subjects even had an accuracy higher than 95%, and three of the seven patients (P5, P6 and P7) also achieved high accuracy (66%, 70%, and 64%, respectively), which demonstrated the effectiveness of our BCIs in communication. Our experimental results for the healthy subjects showed that the hybrid system outperformed the single-modal systems based on only P300 or SSVEPs, whereas the experimental results for DOC patients indicated the possibility of our system in consciousness detection and communication.

It should be noted that these negative results cannot be used as strong evidence for the lack of communication abilities in DOC patients, as the ability of DOC patients to fixate their gaze is usually lacking or insufficient, which is necessary in the use of BCIs based on visual P300 and SSVEP responses. However, the positive results do indicate that the patients are able to communicate with these asynchronous BCIs, so the communication capabilities are there. Therefore, our findings have potential clinical implications for the communication of patients with DOC.

Among the seven patients in this study, although P5 scored 0 on the CRS-R communication subscale before the experiment, the accuracy he obtained in the BCIs was significantly higher than that of chance, which means that he may understand these situations questions and answer correctly through our BCI system. Through follow-up visits, we learned that this patient recovered from the condition and showed motor-dependent behavioral communication two months later. The score of the CRS-R communication sub-scale of Patient P6 after our experiment was also improved compared with that before the experiment (a score of 2). In the year before our experiment, the two MCS patients (i.e. P5 and P6) never showed any clinical motor signs of command-following. This finding demonstrated that BCIs could provide more sensitive diagnostic results for cognitive motor dissociation patients, who are defined as patients who show no detectable command-following behaviors but from whom there is clear neuroimaging evidence of commanding-following brain activities [36].

The ERP waveforms of these patients (P5, P6, and P7) showed that the target stimuli elicited an obvious P300 response (figure 6), and the evocation of SSVEP could be observed on P5 and H1 (figure 7(A)). P300 responses involve sequential activation of the cortical network and depend on higher-order cognitive abilities. It is worth noting that the evoked potential (P300 or SSVEP) of patients was significantly different from those of healthy subjects. For example, patients have a longer P300 latency than healthy subjects (figure 6). However, the P300 amplitude elicited in the patients was significantly lower than that in the control group, as reported in another study [37]. The P300 responses observed in the patients (P3 and P4) suggested that they possessed residual cognitive function. Furthermore, neither P6 and P7's SSVEPs were as apparently evoked as in the healthy control (H1), but their P300s were obviously elicited. The main reason may be that the level of consciousness of DOC patients fluctuates over time, as low levels of consciousness impede the efficient elicitation of SSVEP.

The significant accuracy of BCI in the subjects implied that our approach is effective for communication between patients and the external environment. In this study, we introduced two approaches to improve the performance of BCIs. First, we introduced a two-layer data fusion method to fuse P300 and SSVEP signals. As shown in table 1, 9 of 11 healthy subjects achieved significantly higher accuracies in the hybrid system than in the P300-only or SSVEP-only system. Second, we used a Bayesian framework to dynamically collect the experimental data. The state of the subject was divided into the control state and the idle state. If the subject was focusing on the target, this period was called the control state; otherwise, it was called the idle state. Furthermore, a threshold was applied to discriminate the control and idle states. In our previous work [13], the experimental time for each trial was fixed, and each subject, whether a patient or healthy subject, was asked to complete the experiment in each trial in five rounds (total 10 s). However, the attention and cognitive abilities of DOC patients are weaker than those of healthy subjects, resulting in the patients being prone to fatigue. Therefore, the experimental procedure should be as short as possible. Regarding dynamic stopping in patients, we found that using the Bayesian framework in the patient group, an average of 3.93

rounds was required in each trial. Specifically, there was a 21% reduction in the average number of rounds needed between experiments and a reduction of 105 s in the online experiment. The variable duration in this BCI system depended on the subjects' condition in the testing phase and the thresholds obtained in the training phase. The BCI system used in the online experiment could detect if the user is intending to input commands at all instead of expecting the user to issue one command at every fixed interval throughout the experiment. This conforms to the definition of the asynchronous BCI system, and it is more suitable and effective for the communication of DOC patients.

This study has some limitations. One is that the accuracies of the online experiment for patients were significantly lower than the accuracies for healthy subjects due to the suboptimal EEG signal quality, which may be caused by movement, ocular and respiration artifacts in patients [20]. The second limitation is that only two squares (yes/no) were presented on the screen. The answers limit the type of questions, which limits the practicality of the system. Another limitation of this study is the small number of subjects; only seven patients participated in our study, which affects the generalizability of the results.

For a long time, the lack of communication in DOC patients has seriously affected their diagnosis and prognosis. Our study demonstrated that BCI may provide a novel communication channel for patients with DOC. This study is the first to test hybrid asynchronous BCI in challenging DOC patients. Our results showed that the average number of rounds in the asynchronous system was reduced, thereby shortening the total experiment time for the patients. The significant accuracies of the patients indicate that DOC patients were able to perform simple communication with this BCI system. To further improve the communication tool between DOC patients and BCI, in future studies, we plan to add a third option of 'do not know' on the basis of 'Yes' and 'No' and will develop a practical communication system with a larger number of subjects.

Data availability statement

The data that support the findings of this study are available upon reasonable request from the authors.

Acknowledgments

We sincerely thank the patients and their families for participating in our experiment. This work was supported in part by the Key R&D Program of Guangdong Province (2018B030339001), the Guangzhou Science and Technology Plan Project Key Field R&D Project (202007030005), the National Natural Science Foundation of China (61876067 and 61906019), the Guangdong Natural Science Foundation of China (2019A1515011375), the Guangdong Basic and Applied Basic Research Foundation (2019A1515110388), and the Hunan Provincial Natural Science Foundation (2019JJ50649).

ORCID iD

Jiahui Pan https://orcid.org/0000-0002-7576-6743

References

[1] Jennett B 2002 *The Vegetative State* (London: BMJ Publishing Group Ltd)
[2] Johnson L S M and Lazaridis C 2018 The sources of uncertainty in disorders of consciousness *AJOB Neurosci.* **9** 76–82
[3] Plum F and Posner J B 1982 *The Diagnosis of Stupor and Coma* vol 19 (Oxford: Oxford University Press)
[4] Giacino J T, Ashwal S, Childs N, Cranford R, Jennett B, Katz D I, Kelly J P, Rosenberg J H, Whyte J and Zafonte R D 2002 The minimally conscious state: definition and diagnostic criteria *Neurology* **58** 349–53
[5] Jennett B and Plum F 1972 Persistent vegetative state after brain damage: a syndrome in search of a name *Lancet* **299** 734–7
[6] Giacino J T, Kalmar K and Whyte J 2004 The JFK Coma Recovery Scale-Revised: measurement characteristics and diagnostic utility *Arch. Phys. Med. Rehabil.* **85** 2020–9
[7] Schnakers C, Vanhaudenhuyse A, Giacino J, Ventura M, Boly M, Majerus S, Moonen G and Laureys S 2009 Diagnostic accuracy of the vegetative and minimally conscious state: clinical consensus versus standardized neurobehavioral assessment *BMC Neurol.* **9** 35
[8] Gosseries O, Zasler N D and Laureys S 2014 Recent advances in disorders of consciousness: focus on the diagnosis *Brain Injury* **28** 1141–50
[9] van Erp W S, Lavrijsen J, van de Laar F A, Vos P E, Laureys S and Koopmans R 2014 The vegetative state/unresponsive wakefulness syndrome: a systematic review of prevalence studies *Eur. J. Neurol.* **21** 1361–8
[10] Wang J, Hu X, Hu Z, Sun Z, Laureys S and Di H 2020 The misdiagnosis of prolonged disorders of consciousness by a clinical consensus compared with repeated coma-recovery scale-revised assessment *BMC Neurol.* **20** 1–9
[11] Foster C 2019 It is never lawful or ethical to withdraw life-sustaining treatment from patients with prolonged disorders of consciousness *J. Med. Ethics* **45** 265–70
[12] Pan J, Xie Q, Qin P, Chen Y, He Y, Huang H, Wang F, Ni X, Cichocki A and Yu R 2020 Prognosis for patients with cognitive motor dissociation identified by brain-computer interface *Brain* **143** 1177–89
[13] Pan J, Xie Q, He Y, Wang F, Di H, Laureys S, Yu R and Li Y 2014 Detecting awareness in patients with disorders of consciousness using a hybrid brain–computer interface *J. Neural. Eng.* **11** 056007
[14] Wang F, He Y, Qu J, Xie Q, Lin Q, Ni X, Chen Y, Pan J, Laureys S and Yu R 2017 Enhancing clinical communication assessments using an audiovisual BCI for patients with disorders of consciousness *J. Neural. Eng.* **14** 046024
[15] Zhang H, Guan C and Wang C 2008 Asynchronous P300-based brain–computer interfaces: a computational approach with statistical models *IEEE Trans. Biomed. Eng.* **55** 1754–63
[16] Mason S G and Birch G E 2000 A brain-controlled switch for asynchronous control applications *IEEE Trans. Biomed. Eng.* **47** 1297–307
[17] Millan J R and Mouriño J 2003 Asynchronous BCI and local neural classifiers: an overview of the adaptive brain interface project *IEEE Trans. Neural. Syst. Rehabil. Eng.* **11** 159–61
[18] Townsend G, Graimann B and Pfurtscheller G 2004 Continuous EEG classification during motor

imagery-simulation of an asynchronous BCI *IEEE Trans. Neural. Syst. Rehabil. Eng.* **12** 258–65
[19] Cruse D, Chennu S, Chatelle C, Bekinschtein T A, Fernández-Espejo D, Pickard J D, Laureys S and Owen A M 2011 Bedside detection of awareness in the vegetative state: a cohort study *Lancet* **378** 2088–94
[20] Lulé D, Noirhomme Q, Kleih S C, Chatelle C, Halder S, Demertzi A, Bruno M-A, Gosseries O, Vanhaudenhuyse A and Schnakers C 2013 Probing command following in patients with disorders of consciousness using a brain–computer interface *Clin. Neurophysiol.* **124** 101–6
[21] Pfurtscheller G, Allison B Z, Bauernfeind G, Brunner C, Solis Escalante T, Scherer R, Zander T O, Mueller-Putz G, Neuper C and Birbaumer N 2010 The hybrid BCI *Front. Neurosci.* **4** 3
[22] He M, Horng S-J, Fan P, Run R S, Chen R-J, Lai J L, Khan M K and Sentosa K O 2010 Performance evaluation of score level fusion in multimodal biometric systems *Pattern Recognit.* **43** 1789–800
[23] Long J, Li Y, Yu T and Gu Z 2011 Target selection with hybrid feature for BCI-based 2D cursor control *IEEE Trans. Biomed. Eng.* **59** 132–40
[24] Yin E, Zeyl T, Saab R, Chau T, Hu D and Zhou Z 2015 A hybrid brain–computer interface based on the fusion of P300 and SSVEP scores *IEEE Trans. Neural. Syst. Rehabil. Eng.* **23** 693–701
[25] Jasper H H 1958 The ten-twenty electrode system of the International Federation *Electroencephalogr. Clin. Neurophysiol.* **10** 370–5
[26] Chang C C and Lin C J 2011 LIBSVM: a library for support vector machines *ACM Trans. Intell. Syst. Technol.* **2** 1–27
[27] Chen X, Wang Y, Nakanishi M, Jung T P and Gao X 2014 Hybrid frequency and phase coding for a high-speed SSVEP-based BCI speller *2014 36th Annual Int. Conf. IEEE Engineering in Medicine and Biology Society* (IEEE) pp 3993–6
[28] Zhang Y, Zhou G, Jin J, Wang X and Cichocki A 2015 SSVEP recognition using common feature analysis in brain–computer interface *J. Neurosci. Methods* **244** 8–15
[29] Zhang Y, Zhou G, Jin J, Wang X and Cichocki A 2014 Frequency recognition in SSVEP-based BCI using multiset canonical correlation analysis *Int. J. Neural. Syst.* **24** 1450013
[30] Lin Z, Zhang C, Wu W and Gao X 2006 Frequency recognition based on canonical correlation analysis for SSVEP-based BCIs *IEEE Trans. Biomed. Eng.* **53** 2610–4
[31] Nakanishi M, Wang Y, Wang Y T, Mitsukura Y and Jung T P 2014 A high-speed brain speller using steady-state visual evoked potentials *Int. J. Neural. Syst.* **24** 1450019
[32] Miller I, Miller M and Freund J E 2014 *John E. Freund's Mathematical Statistics with Applications* (Boston: Pearson)
[33] Serby H, Yom-Tov E and Inbar G F 2005 An improved P300-based brain-computer interface *IEEE Trans. Neural. Syst. Rehabil. Eng.* **13** 89–98
[34] Noble W S 2006 What is a support vector machine? *Nat. Biotechnol.* **24** 1565–7
[35] Kübler A and Birbaumer N 2008 Brain–computer interfaces and communication in paralysis: extinction of goal directed thinking in completely paralysed patients? *Clin. Neurophysiol.* **119** 2658–66
[36] Schiff N D 2015 Cognitive motor dissociation following severe brain injuries *JAMA Neurol.* **72** 1413–5
[37] Wang X, Wu H, Lu H, Huang T, Zhang H and Zhang T 2017 Assessment of mismatch negativity and P300 response in patients with disorders of consciousness *Eur. Rev. Med. Pharmacol. Sci.* **21** 4896–906